ISSUE: April 2024

Designing An Open-Source Power Inverter (Part 16): Transformer Winding Design For the Battery Converter—Efficiency Range And Winding Allotment

by Dennis Feucht, Innovatia Laboratories, Cayo, Belize

As this Volksinverter design series[1-15] moves forward, we continue the presentation of the transformer design procedure for boost push-pull (BPP) power-transfer circuits. As with other discussions in this series, this procedure applies both to a specific component in the Volksinverter design—the transformer in the battery converter stage's power transfer circuit (see Figs. 1 and 2), and more generally to other similar designs. The transformer design procedure presented here, may also be applied more broadly to other transformer designs in switched-mode power supplies, particularly low-R_g converters such as point-of-load (POL) converters.

While the recent part 15 of this series discussed core selection, this part addresses another aspect of the magnetics design—winding area allocation. This represents the first part of the electrical (winding) design (Fig. 3).

The criteria for winding design are maximum power transfer across windings (primary to secondary) over a specified current range, optimal winding loss, and spatially uniform loss distribution. The discussion in this part determines the electrical parameters of the windings that will produce maximum power transfer, given the core selection and the circuit's operating conditions. The formulas derived here will allow us to determine wire sizes and winding configurations in the next part.

Transformer winding (electrical) design is usually more complicated than core (magnetic) design because cores have already been designed by core manufacturers, and magnetic design largely consists of core selection. Although the same can be said of round plastic-coated magnet wire, wire sizes span a wider range than core sizes, and wire bundle strand configurations portend even greater possibilities.

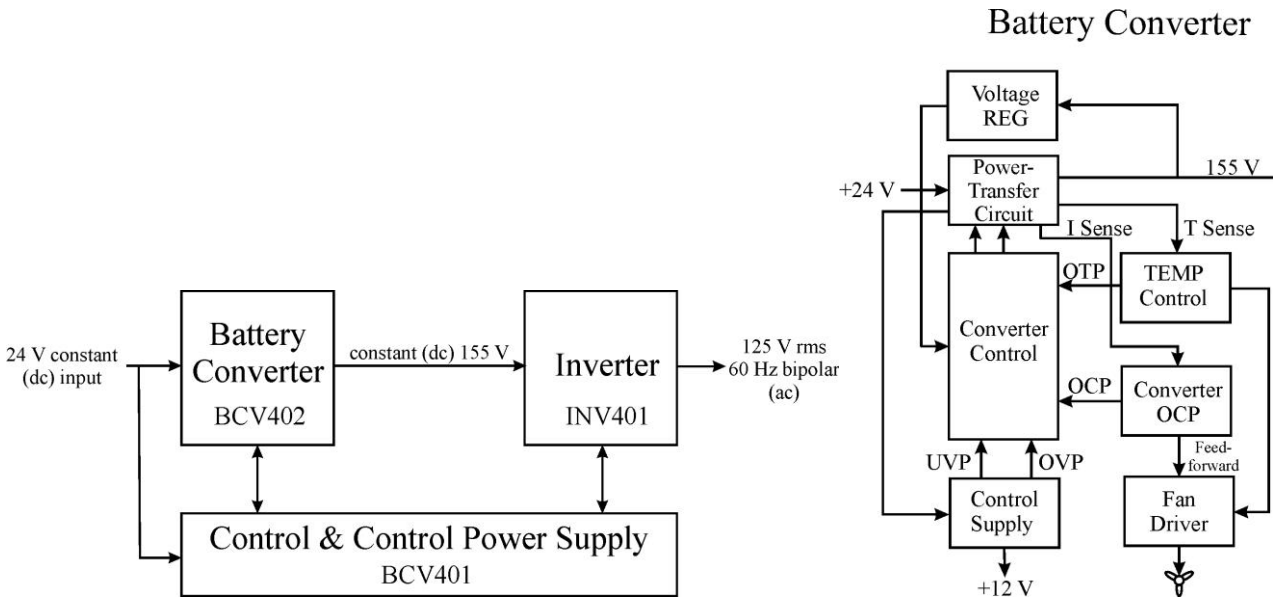

Fig. 1. The Volksinverter's system block diagram (left) and the BCV402 battery converter stage block diagram (right).

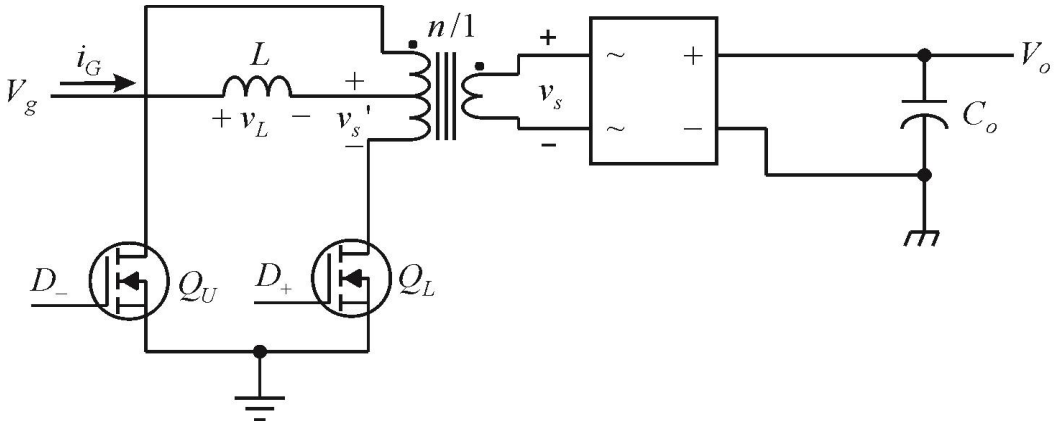

Fig. 2. The CA (boost) push-pull power-transfer circuit (BPP).

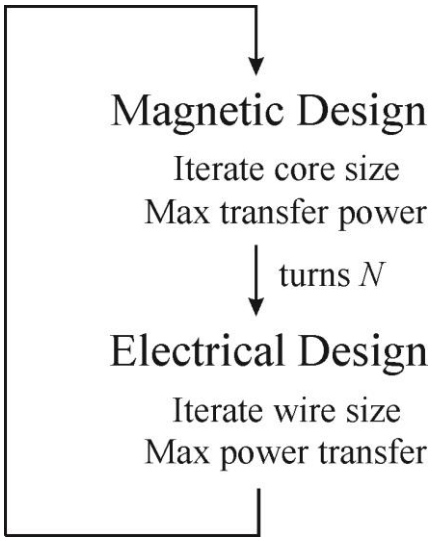

Fig. 3. General procedure for transductor (multi-winding magnetic component) design: magnetic design chooses core size to maximize transfer-power density; then winding design maximizes power transfer across windings.

Optimal Efficiency Over Current Range

Fig. 4 graphs efficiency curves for primary-to-secondary winding power transfer versus primary current scaled as a fraction of its full-scale or fs (short-circuit secondary) V_p/R_w value. At zero output voltage the secondary port has zero power at a maximum current ≈ V_p/R_w, and transfer efficiency $\eta = \overline{P}_s / \overline{P}_p = 0$. An open-circuit output also has zero power near the zero-current extreme of the η range. $\eta(0) \neq 0$ because of core loss (in equivalent core resistance R_c) from magnetizing current.

η_{max} moves left across the Fig. 1 plots as η_{max} increases. On any one plot η decreases from η_{max} more abruptly as current decreases. η decreases above η_{max} (toward the right) nearly linearly with i_p. The choice of η curve depends on parameter β_p. The specified current range [i_{pL}, i_{pH}] corresponds to a scaled-i_{pL} range in Fig. 4.

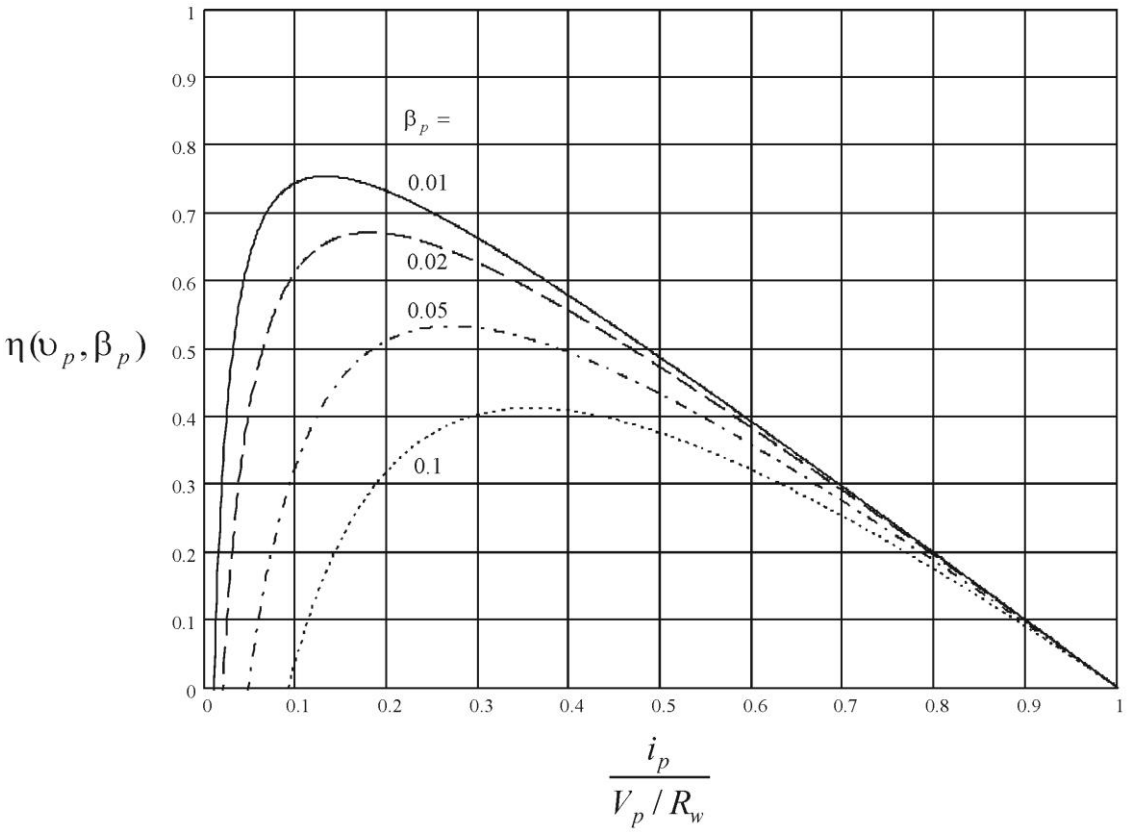

Fig. 4. Winding power-transfer efficiency as a function of primary current, scaled to maximum (secondary short-circuit) value. Increased winding resistance R_{wp} decreases peak efficiency. βp is the primary winding resistance to core resistance ratio, shown lower than for the Volksinverter transformer to exaggerate plot features for easier viewing.

How do we select an efficiency curve $\eta(i_p)$ that has its peak positioned optimally within the primary current i_p range? (At high η, primary-referred secondary current $i_s' \approx i_p$.) Put another way, where within the current range of i_p should peak efficiency $\eta_{max}(i_p)$ occur?

One optimization places the limits of the current range at equal minimum η with η_{max} between them. Then over the current range, η is guaranteed to be greater than the minimum of the current range limits. This choice of η_{max} positioning is optimal for current that is significant over the whole range where low η at minimum $i_p = i_{pL}$ is as important as at maximum $i_p = i_{pH}$. However, power transfer is lowest at i_{pL} as is power loss, and $\eta(i_{pL})$ is not as important to maintain as at full-scale power transfer of $\eta(i_{pH})$.

Another alternative is to position η_{max} around the mid-scale value of V_g and hence of $\tilde{i}_p$. Yet another is to set $\eta(i_{pH}) = \eta_{max}$. By placing the fs current at η_{max} at the right end of the range in Fig. 4, the range is then to the left of η_{max} along the abrupt down-slopes of the η curves, with maximum variation in η over the current range.

However, this results in low η at zero-scale or zs current. Inverters typically operate near zs current for long periods of time such as at night, and if η is very low they can accrue substantial loss in energy and battery charge at low power. Consequently, an optimal η_{max} for off-grid inverter design positions η_{max} somewhere within the load-current range.

The independent variable of $\eta(i_p, \beta_p)$ is i_p. The other parameter, β_p, is the primary-winding-to-core resistance ratio

$$\beta_p = R_{wp}/R_c \text{ , } R_w = R_{wp} + R_{ws}'$$

scaled to the primary-referred core resistance R_c of the transformer circuit model.[16] Each curve of Fig. 4 has a fixed β_p value as parameter and as β_p decreases, the curve peaks rise upward and to the left. By setting the winding referral ratio to the turns-ratio $n = N_p/N_s$, the secondary winding resistance is referred to either of the primary windings and splits equally between them as $R_{wp} = R_{ws}'$. Then $R_w = 2 \cdot R_{wp}$ or $R_{wp} = ½ \cdot R_w$. Secondary winding loss is set equal to that of the two primary windings together so that the winding-to-core *power-loss ratio* ψ at η_{max} is

$$\psi_{max} \equiv \overline{P}_w / \overline{P}_c = \beta_p + 1 \approx 1 \text{ , } \eta_{max}$$

Each boost push-pull (BPP) primary winding delivers half the transfer power and shares equal winding loss of $\overline{P}_w/2$.

From the magnetic part of the Volksinverter transformer design, in part 15, the parameter that relates core design to winding design for the ETD34-3C90 core is the primary winding turns $N_p = 6$. The primary winding is the reference winding of the design because it inputs the most power. The optimal primary-referred winding resistance from part 15 follows from the core thermal model and maximum (allowed) core power loss;

$$\text{BPP primary per-winding resistance} = R_{wpopt} = \frac{1}{2} \cdot \frac{\psi_{max} \cdot (\overline{P}_c / 2)}{\tilde{i}_p^{\,2}} \approx \frac{0.476\,\text{W}}{\tilde{i}_p^{\,2}} \text{ , } \overline{P}_w \approx \overline{P}_c \text{ at } \psi_{max} \approx \eta_{max} \approx 1, \beta_p \approx 0$$

Winding loss $\overline{P}_w = \psi_{max} \cdot \overline{P}_c = (\beta_p + 1) \cdot \overline{P}_w$ is set nearly equal to core loss $\overline{P}_c$ = 1.9 W to maximize power transfer at $\tilde{i}_p$ around η_{max}. Power is split equally $(\overline{P}_c / 2)$ between primary and secondary windings for uniform winding loss density. Each of the two primary windings is then allotted half (½) of this amount or $\psi_{max} \cdot \overline{P}_c/4$ overall. Maximum $\tilde{i}_p$ over the V_g range is at V_{gmin} = 20 V where D' = 0.500. The Volksinverter with an ETD34 design power goal of 500 W at V_{gmin} = 20 V has a fs RMS primary current followed by the winding resistance as a design goal (*opt*);

$$\tilde{i}_p = \frac{I_g}{2} \cdot \sqrt{1 + D'} = \frac{\overline{P}_g}{V_g} \cdot \frac{\sqrt{1 + 0.500}}{2} \approx \frac{\overline{P}_g}{20\,\text{V}} \cdot (0.612) = \frac{500\,\text{W}}{32.66\,\text{V}} = 15.31\,\text{A} \Rightarrow R_{wpopt} = \frac{0.476\,\text{W}}{(15.31\,\text{A})^2} = 2.03\,\text{m}\Omega \approx 2\,\text{m}\Omega$$

In battery converters of off-grid inverters, load current range is typically two to three decades. For the Volksinverter, the BCV402 ETD34 design range goal is 500 W full-scale (fs) to about 0.5 W to 5 W zero-scale (zs). Over this range, locating η_{max} near fs minimizes fs power loss, though as η_{max} is increased in design by reducing R_{wp}, its position moves nearer to zs. For a current range of 0 to 0.3 on the scaled-current axis of Fig. 4, as R_w (and hence β_p) decreases, the η_{max} peak moves to the left, toward zs current.

The reference [17] design formulas position the efficiency peak η_{max} so that minimum η is the same at the limits of the current range. When applied in the Volksinverter design, additional characteristics of the method are revealed.

The η curves converge at both high and low ends of the current range; to increase the range, lower R_{wp} is required for more-efficient curves with higher η_{max}. For a given minimum η the widest range is achieved by the most efficient curves.

The default choice in the calculation of R_{wpopt} is to place η_{max} near fs current, thereby reducing power loss at fs power. This choice will be continued in the Volksinverter design, though the reader should be aware that if a winding plan results in $R_{wp} > R_{wpopt}$, the η curve of operation has a lower η_{max} and is shifted toward the fs current end of the range.

BPP Winding Losses And Window Winding Allotment

The second task in winding design after choosing the winding configuration is to allot cross-sectional winding areas A_{wx} in the winding window to windings as fractions k_{wx} of the total (bobbin or coil former) window area A_w. In most power-transfer circuits with square-wave (two-level) waveforms, current density in the windings is made uniform by equally dividing primary and secondary winding areas.

Apart from losses, the two winding-current polarities—those of primary and secondary—handle an equal amount of power. Wire sizes are chosen for equal current area density in the windings. Equal winding areas with equal winding loss uniformly distribute heat (but not temperature) in the window. BPP secondary waveforms are two-level square-waves; the primary current waveforms are three-level.

The optimal area allotments with three-level current waveforms are different and we will need to derive them. The two primary windings share equal winding areas of $A_{wp}/2$ in the window winding-area allotment because they are functionally identical, operating the same for opposite halves of the switching cycle. The secondary winding is allotted A_{ws}. Allotment of the total bobbin window area A_w is thus

$$A_{wp} = k_{wp} \cdot A_w \;;\; A_{ws} = k_{ws} \cdot A_w$$

Primary and secondary winding losses are

$$\overline{P}_{wp} = 2 \cdot \tilde{i}_p^{\,2} \cdot R_{wp} = 2 \cdot \left(\frac{I_g}{2} \cdot \sqrt{1 + D'} \right)^2 \cdot R_{wp} = \tfrac{1}{2} \cdot (1 + D') \cdot I_g^2 \cdot R_{wp}$$

$$\overline{P}_{ws} = (n \cdot I_g \cdot \sqrt{D'})^2 \cdot R_{ws} = n^2 \cdot I_g^2 \cdot D' \cdot \left(\frac{R_{wp}}{n^2} \right) = D' \cdot I_g^2 \cdot R_{wp}$$

Secondary winding loss is referred to the primary winding by turns ratio n = ¼ from the magnetic design, and the additional constraint of $R_{ws} = R_{wp}/n^2$ is R_{wp} referred to the secondary winding by n^2; turns ratio n relates primary and secondary wire or bundle turns.

For uniform winding-loss area density, the *winding-area ratio*

$$Y = \frac{A_{wp}}{A_{ws}} = \frac{2 \cdot \tilde{i}_p^{\,2}}{(\tilde{i}_s / n)^2} = \frac{1}{2} \cdot \frac{1 + D'}{D'}$$

$$A_w = A_{wp} + A_{ws} \Rightarrow A_{wp} = A_w - A_{ws} \;;\; \frac{A_{ws}}{A_w} = \frac{1}{Y + 1} \;;\; \frac{A_{wp}}{A_w} = \frac{Y}{Y + 1}$$

The ratio of winding losses is equal to the area ratio;

$$\boxed{\frac{\overline{P}_{wp}}{\overline{P}_{ws}} = \frac{1 + D'}{2 \cdot D'} = Y}$$

The table shows the results over the BPP input voltage range with circuit design parameters from Table 1 of part 15.

Table. Optimal winding areas over V_g range with avg P_g = 333 W.

V_g, V	I_g, A	D'	$Y = \frac{k_{wp}}{k_{ws}} = \frac{1+D'}{2 \cdot D'}$	$k_{wp} = \frac{A_{wp}}{A_w} = \frac{Y}{Y+1}$	$k_{ws} = \frac{A_{ws}}{A_w} = \frac{1}{Y+1}$
20	16.66	0.500	1.50	0.600	0.400
25	13.32	0.625	1.30	0.565	0.435
30	11.1	0.750	1.167	0.538	0.462

Optimal BPP allocations are given as $k_{wp} \cdot A_w$ to the primary windings and $k_{ws} \cdot A_w$ to the secondary winding. The allocation is shown in Fig. 2. The common dimension of w_w relates k_{wp} directly to the height dimension.

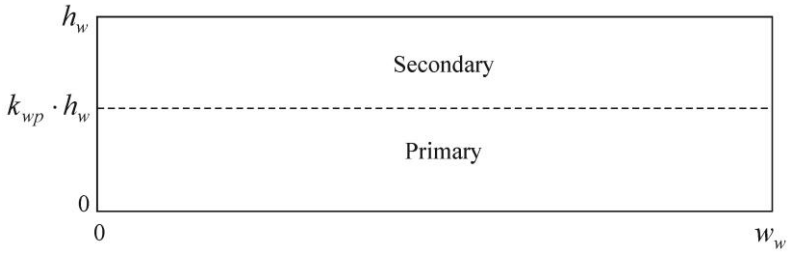

Fig. 5. Cross-sectional area allotments of BPP primary windings have k_{wp} and secondary winding has 1 – k_{wp} = k_{ws}. The core center-leg is beneath the primary area. Primary winding areas are adjusted to maximize packing factor. Area dimensions of the combined primary windings are w_w by $k_{wp} \cdot h_w$.

Winding-loss density varies with duty-ratio as a design parameter and consequently with where we place the operating-point. At the previously determined midrange operating-point, D' = 0.625 and loss-ratio Y = 1.3. The BPP winding loss-ratio Y is graphed in Fig. 6.

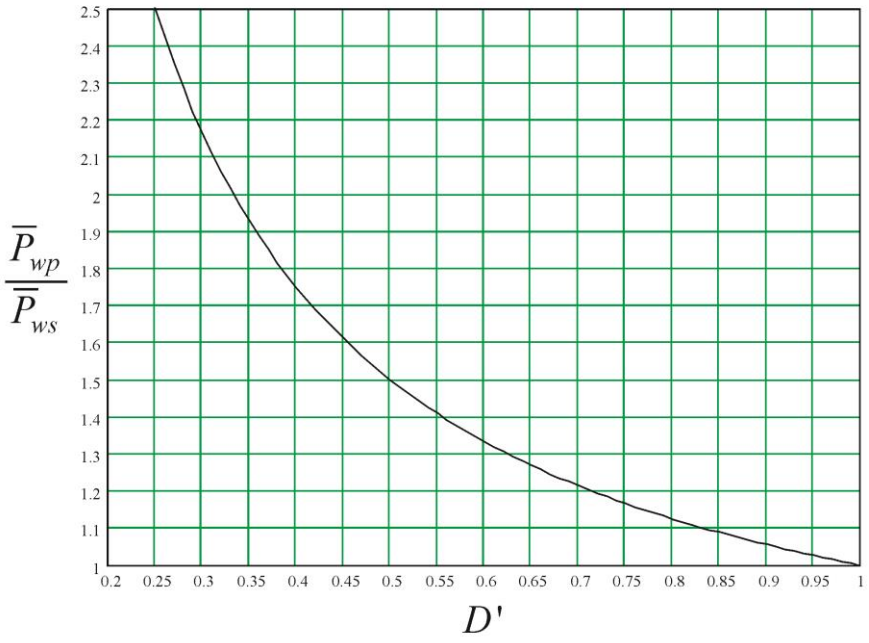

Fig. 6. Ratio of primary-to-secondary winding losses as a function of D' = 1 – D. The midrange value of winding-loss-ratio Y = 1.3 is near the equal-switch-loss value of $D'_{opt} \approx 0.618$.

The value of $D'_{opt} \approx 0.618$, derived in Volksinverter part 11, is optimum for equal active and passive switch loss near midrange.[11] The choice of equal switch-loss at D'_{opt} = 0.618, and V_g = 24.72 V is near midrange

V_g at V_{gmid} = 25 V where Y = 1.3. Winding loss is greatest at maximum current at V_{gmin} = 20 V. Consequently, the winding areas have been allotted for optimal areas at the greatest winding loss; $Y(V_{gmin}) = Y_{min}$ = 1.50 and k_{wp} = 0.6 is chosen as the winding area allotment. Then over the operating range, $Y < Y_{min}$, and the secondary winding has greater power loss than that of the primary.

Area allocation based on uniform power-loss density does not necessarily accomplish the goal of equal winding temperatures. The secondary winding is adjacent to surrounding air and is cooled by it to a lower temperature than the primary winding buried beneath it and conducting heat from core loss of the center leg. However, most of the heat from the primary winding and core beneath it will exit to ambient through the secondary winding, heating it more than it heats itself.

Copper thermal conductivity is about 95 times that of ferrite core material. Windings have $k_{px} \cdot A_{wx}$ of copper area with the rest being air and wire insulation. Even so, windings consisting of air and insulation interspersed with conductor are much more thermally conductive than core material and have less ΔT across them for the same heat flow.

A more rigorous thermal design of the transformer would include secondary thermal conduction of both $\overline{P}_{ws}$ and $\overline{P}_{wp}$ through the secondary winding. With the secondary winding closest to ambient, the two effects oppose for temperature rise, and for this design, only the uniform power-loss density criterion at maximum winding loss is chosen for $Y = Y_{min}$.

Static Winding Current And Power

Magnetics design has two thermal models, one for the core (in Volksinverter Part 15) and one for the winding. The *winding thermal model* is the wire ampacity density $\tilde{J}_0$ scaled by [18]

$$\text{Wire current-density thermal size factor} = \tilde{J} / \tilde{J}_0 = (A \cdot A_w / \text{cm}^4)^{-1/8},\ \tilde{J}_0 = 4.5\ \text{A/mm}^2,\ 25\ ^\circ\text{C, Cu}$$

(*Ampacity* is a wire static (0 Hz) current limit.) The factor is scaled for $\tilde{J} / \tilde{J}_0$ = 1 at $A \cdot A_W$ = 1 cm^4. As cores increase in size, heat is buried more deeply in the larger windings and internal temperature rises. $\tilde{J} / \tilde{J}_0$ thermally adjusts allowable current density for winding size. Then for an ETD34 core size (for which $A \cdot A_W$ = 1.194 cm^4), $\tilde{J} / \tilde{J}_0$ = 0.978.

An ETD34 horizontal Ferroxcube bobbin has A_W = 123 mm^2. The maximum static field current in a conductor-filled winding window (for Cu wire) and an ETD34 core size constrained by the winding thermal equation is

$$NI_w = (\tilde{J} / \tilde{J}_0) \cdot \tilde{J} \cdot A_w = (0.978) \cdot (4.5\ \text{A/mm}^2) \cdot (123\ \text{mm}^2) = 541\ \text{A}$$

NI_w designates a constant current though it results from RMS current $\tilde{J} \cdot A_w$ as the equivalent static current that would cause the same amount of heating. (The RMS value of constant current is its constant value.)

Large wire has the required ampacity for the primary winding but large-size (high-ξ_r) winding solutions are uncommon (as we will see in part 17); multiple strands of smaller wire are common, twisted into a bundle. Round strands within a bundle pack the same as round bundles to each other.

Then for the least (worst-case) k_p layer configuration, layers are aligned, and intrabundle packing $k_{pb} = k_{pf}$ = 0.7854. Twisting enlarges a bundle, resulting in a conductive bundle cross-sectional area expansion of k_{tw}. An initial estimate can be made of packing factor as

$$k_p = k_{pf} \cdot k_{pb} \cdot k_{pw} \cdot k_{tw} = (0.7854) \cdot (0.7854) \cdot (0.856) \cdot (0.98) = 0.517\ ,\ k_{pw}(\#\ 17) = 0.856$$

Wire size of #17 AWG is a guess, needed to approximate a value for k_p. This is only an estimate because we have not yet determined wire size, and p*orosity* k_{pw} varies with round-wire size, from 0.910 for #8 AWG wire to 0.581 for #42. It reduces conductor area as insulation spacing between adjacent wires.

The estimated maximum static primary RMS current with these geometric winding constraints is

$$\text{Primary current (each side)} = \tilde{i}_p = \frac{\frac{1}{2}\cdot k_{wp}\cdot NI_w\cdot k_p}{N_p} = \frac{(0.3)\cdot(541\,\text{A})\cdot(0.517)}{6} = \frac{83.91\,\text{A}}{6} = 13.98\,\text{A}$$

This estimated current is a maximum theoretical value that falls short of the value (page 4, middle) required for a design power of 500 W:

$$\tilde{i}_p = \frac{I_g}{2}\cdot\sqrt{1+D'} = \frac{\overline{P}_g}{V_g}\cdot\frac{\sqrt{1+0.500}}{2} \approx \frac{\overline{P}_g}{20\,\text{V}}\cdot(0.612) = \frac{500\,\text{W}}{32.66\,\text{V}} = 15.31\,\text{A}$$

The most power that can be expected is found by solving this equation for $\overline{P}_g$ and substituting $\tilde{i}_p$ = **13.98 A**;

$$\overline{P}_g \le V_g\cdot\tilde{i}_p\cdot\frac{2}{\sqrt{1+D'}} = (20\text{ V})\cdot(13.98\text{ A})/(0.612) = \mathbf{457\ W}$$

The winding resistance goal for this design power is

$$R_{wpopt} = \frac{0.476\,\text{W}}{\tilde{i}_p^{\,2}} = \frac{0.476\,\text{W}}{(13.98\,\text{A})^2} = \mathbf{2.44\ m\Omega}$$

Maximum BPP input (inductor) current is

$$I_{g\max} = \frac{2}{\sqrt{1+D'_{\min}}}\cdot\tilde{i}_p \approx (1.633)\cdot\tilde{i}_p = \mathbf{22.83\ A}$$

The no-loss maximum static secondary current and power are

$$\max\ \bar{i}_s = n\cdot D'_{\min}\cdot I_{g\max} = (1/4)\cdot(0.500)\cdot I_{g\max} = (0.125)\cdot I_{g\max} = 2.85\text{ A} \Rightarrow \overline{P}_{s0}' = (160\text{ V})\cdot\bar{i}_s = 457\text{ W}$$

With no power loss in winding transfer, $\overline{P}_{g0} = \overline{P}_{s0}'$ because the max $\bar{i}_s$ equation is based on the transfer function; substitute $V_{g\min} = n\cdot D'_{\min}$ and the two power-loss expressions are equal.

The packing factor of secondary winding layers is based on another guess for k_{pw}, and assuming no bundling (single strand, k_{pb} = 1, k_{tw} = 1) is

$$k_{ps} = k_{pf}\cdot k_{pb}\cdot k_{pw}\cdot k_{tw} = (0.7854)\cdot(1)\cdot(0.799)\cdot(1) = 0.628,\ k_{pw}(\#\,24.5) = 0.799$$

The maximum achievable secondary RMS current is thus

$$\max\ \tilde{i}_s = \frac{k_{ws}\cdot k_{ps}\cdot NI_w}{N_p\cdot(1/n)} = \frac{(0.4)\cdot(0.628)\cdot(541\,\text{A})}{6\cdot 4} = \frac{135.9\,\text{A}}{24} = \mathbf{5.66\ A}$$

The secondary winding can handle an output power at a constant V_o = 160 V, by Watt's Law, of V_o multiplied by the maximum average current (where $D'_{\min} = 0.5 = D'$ at $V_{g\min}$ = 20 V),

$$\max\ \bar{i}_s = \tilde{i}_s \cdot \sqrt{D'_{\min}} = (5.66\ \text{A})\cdot(0.707) = 4.00\ \text{A} \Rightarrow \bar{P}_{s0} = (160\ \text{V})\cdot\bar{i}_s = 640\ \text{W}$$

Secondary power $\bar{P}_{s0}$ is significantly greater than the primary power referred to the secondary as $\bar{P}_{s0}'$. The discrepancy between the two $\bar{P}_{s0}$ values is the factor 640 W/457 W = 1.40. It is expressed at $V_{g\min}$ by the ratio

$$\frac{\bar{P}_{s0}}{\bar{P}_{s0}'} = \frac{\sqrt{D'_{\min}}}{\left(\frac{D'_{\min}}{\sqrt{1+D'_{\min}}}\right)}\cdot\frac{k_{ws}}{k_{wp}}\cdot\frac{k_{ps}}{k_{pp}} = \left(\sqrt{\frac{1+D'_{\min}}{D'_{\min}}}\right)\cdot\left(\frac{1}{Y}\right)\cdot\left(\frac{k_{ps}}{k_{pp}}\right) = \left(\sqrt{\frac{1+D'_{\min}}{D'_{\min}}}\right)\cdot\left(\frac{2\cdot D'_{\min}}{1+D'_{\min}}\right)\cdot\left(\frac{k_{ps}}{k_{pp}}\right) \Rightarrow$$

$$\frac{\bar{P}_{s0}}{\bar{P}_{s0}'} = \left(2\cdot\sqrt{\frac{D'_{\min}}{1+D'_{\min}}}\right)\cdot\left(\frac{k_{ps}}{k_{pp}}\right) = (1.155)\cdot(1.215) = 1.40,\ \text{min}\ V_g = 20\ \text{V}$$

At midrange, it is (1.240)·(1.215) = 1.51. This shows that the secondary winding can transfer more power than the primary winding because both factors in the secondary power ratio are greater than one. The second factor is from a higher k_p of the secondary turns because its k_{pb} = 1 is a single strand of wire; the first factor exceeds one because of the difference in primary and secondary current waveshapes. Also, power loss increases by the square of current while transfer power is linear with i_s (because V_s is held constant). Consequently, the additional secondary area required for uniform winding loss gives the secondary more transfer power capability. This tends to compensate for primary heat loss through the secondary winding.

These design formulas give the winding area and resistance as parameters for proceeding to the design of the primary and secondary windings, continued in the second part of the converter transformer winding design.

References

1. "Designing An Open-Source Power Inverter (Part 1): Goals And Specifications" by Dennis Feucht, How2Power Today, May 2021.
2. "Designing An Open-Source Power Inverter (Part 2): Waveshape Selection" by Dennis Feucht, How2Power Today, September 2021.
3. "Designing An Open-Source Power Inverter (Part 3): Power-Transfer Circuit Options" by Dennis Feucht, How2Power Today, April 2022.
4. "Designing An Open-Source Power Inverter (Part 4): The Optimal Power-Line Waveshape" by Dennis Feucht, How2Power Today, May 2022.
5. "Designing An Open-Source Power Inverter (Part 5): Kilowatt Inverter Circuit Design" by Dennis Feucht, How2Power Today, July 2022.
6. "Designing An Open-Source Power Inverter (Part 6): Kilowatt Inverter Control Circuits" by Dennis Feucht, How2Power Today, August 2022.
7. "Designing An Open-Source Power Inverter (Part 7): Kilowatt Inverter Magnetics" by Dennis Feucht, How2Power Today, September 2022.
8. "Designing An Open-Source Power Inverter (Part 8): Converter Control Power Supply" by Dennis Feucht, How2Power Today, November 2022.
9. "Designing An Open-Source Power Inverter (Part 9): Magnetics For The Converter Control Power Supply" by Dennis Feucht, How2Power Today, December 2022.
10. "Designing An Open-Source Power Inverter (Part 10): Converter Protection Circuits" by Dennis Feucht, How2Power Today, February 2023.
11. "Designing An Open-Source Power Inverter (Part 11): Minimizing Switch Loss In Low-Input-Resistance Converters" by Dennis Feucht, How2Power Today, March 2023.

12. "Designing An Open-Source Power Inverter (Part 12): Sizing The Converter Magnetics" by Dennis Feucht, How2Power Today, March 2023.

13. "Designing An Open-Source Power Inverter (Part 13): The Differential Boost Push-Pull Power-Transfer Circuit" by Dennis Feucht, How2Power Today, June 2023.

14. "Designing An Open-Source Power Inverter (Part 14): Boost Push-Pull Or Buck Bridge?" by Dennis Feucht, How2Power Today, July 2023

15. "Designing An Open-Source Power Inverter (Part 15): Transformer Magnetic Design For the Battery Converter" by Dennis Feucht, How2Power Today, March 2024.

16. "Optimizing Transformer Winding Design For Max Efficiency Over Output Current Range" by Dennis Feucht, How2Power Today, September 2018.

17. "Maximizing Power Transfer Efficiency Over A Current Range" by Dennis Feucht, How2Power Today, December 2023.

18. "Magnetics Optimization (Part 3): Maximum Power Transfer Of Magnetics Circuit Model" by Dennis Feucht, How2Power Today, April 2017.

19. "How Wire Bundle Configurations Influence Eddy-Current Proximity Effects" by Dennis Feucht, How2Power Today, February 2019.

20. "How Twisted Bundles Reduce Eddy-Current Effects In Winding Bundle Design" by Dennis Feucht, How2Power Today, September 2023.

About The Author

Dennis Feucht has been involved in power electronics for 40 years, designing motor-drives and power converters. He has an instrument background from Tektronix, where he designed test and measurement equipment and did research in Tek Labs. He has lately been working on projects in theoretical magnetics and power converter research.

For more on magnetics design, see these How2Power Design Guide search results.